Discussion

During the past few years several developments have shown that there is a great deal of unpredictability, even randomness, in the application of direct methods. *MULTAN* was devised in the first place to provide an objective and therefore programmable procedure for solving crystal structures. Much time and effort have been expended in designing systematic procedures for obtaining good starting points (convergence) and good phase extension (weighted tangent formulae). In the event, for complex structures, *MULTAN* is sometimes made to give a solution by imposing some quite arbitrary and irrational change in the systematic procedure – by artificially halving or doubling the temperature factor, for example.

The message that emerges is this – that the greater the number of different processes or pathways that can be provided in the phase-determining procedure the greater is the chance of success. Here, in the development of *MAGEX*, there are alternative functions for parameter-shift refinement, one of them seemingly more effective but also more expensive, and also alternative ways of handling special reflexions. A clear preference for the latter process cannot be given. In fact there is little point in trying to provide quantitative comparisons between one procedure and another – at any rate for the ones described here. There is far too great a variation in their performance from one structure to another to make the exercise worthwhile.

These alternatives are included as standard components of *MAGEX*80 which is run with *MULTAN*80, the current version of that program. Our experience shows that *MAGEX*80 is certainly more effective than both the original *MAGIC* program and also the first version of *MAGEX*. Indeed we have an impression from numbers of tests that it may be somewhat more effective than any other procedure devised and distributed by the York/Louvain group.

This project has received generous support from the Science and Engineering Research Council. One of us (ZSH) gratefully acknowledges the support of the British Council and of the Ministry of Education of the People's Republic of China. Discussions with Dr J. P. Declercq and Dr G. Germain of the University of Louvain have also contributed to the success of the work here described. We also wish to express our thanks to Dr I. L. Karle for the kind provision of the guainolide data.

References

HULL, S. E., VITERBO, D., WOOLFSON, M. M. & ZHANG SHAO-HUI (1981). *Acta Cryst.* A**37**, 566–572.

POSNER, G. H., BABIAK, K. A., LOOMIS, G. L., FRAZEE, W. J., MITTAL, R. A. & KARLE, I. L. (1981). *J. Am. Chem. Soc.* In the press.

WATKIN, D. (1981). Private communication.

Acta Cryst. (1982). A**38**, 685–694

High-Resolution Electron Microscopy of McGillite. I. One-Layer Monoclinic Structure

BY SUMIO IIJIMA*

Center for Solid State Science, Arizona State University, Tempe, Arizona 85287, *USA*

(*Received* 15 *September* 1981; *accepted* 19 *April* 1982)

Abstract

The crystal structure of mcGillite from Sullivan mine, Kimberley, Canada, which has been described as the fifth member of the pyrosmalite family, has been studied using electron diffraction and high-resolution electron microscopy. A new monoclinic structure for this mineral is proposed with $a = \sqrt{3}a_0 = 23{\cdot}279$, $b = a_0 = 13{\cdot}498$, $c = c_0/\sin\beta = 7{\cdot}390$ Å, $\beta = \tan^{-1}(\sqrt{3}a_0/12c_0) = 105{\cdot}3°$, where $a_0 = 13{\cdot}498$, $c_0 = 85{\cdot}657/12 = 7{\cdot}138$ Å for the trigonal cell proposed by Donnay, Betournay & Hamill [*Can. Mineral.* (1980), **18**, 31–36]. The space group is $C2/m$. The crystal is considerably disordered, which results from frequent occurrences of the 120° rotation twinning about [100]. Some of these twins have a thickness of only one unit cell. It is proposed that crystal structures of other members of manganpyrosmalites whose structures are reported as rhombohedral or hexagonal should be

* Present address: Research and Development Corporation of Japan, Department of Physics, Meijo University, Yagoto-Urayama, Tenpaku-ku, Nagoya, Japan.

0567-7394/82/050685-10$01.00

reexamined in terms of the one-layer monoclinic structure.

1. Introduction

Frondel & Bauer (1953) reported the mineral manganpyrosmalite $(Mn,Fe)_8(Si_6O_{15})(OH,Cl)_{10}$, as being hexagonal and isostructural with pyrosmalite $(Fe,Mn)_8(Si_6O_{15})(OH,Cl)_{10}$. The crystal structure of this silicate mineral was briefly reported by Takéuchi, Kawada & Sadanaga (1963) and its structure was later refined (Takéuchi, Kawada & Sadanaga, 1969; Kashaev, 1968). According to these X-ray diffraction studies on single crystals of manganpyrosmalite its crystal structure is categorized as a sheet silicate consisting of sheets of SiO_4 tetrahedra having a configuration $(Si_6O_{15})^{6-}$ and sheets of pyrochroite $Mn(OH)_2$. These layers are stacked alternately in the c-axis direction.

Schallerite and friedelite have very similar formulae to that of manganpyrosmalite. Their X-ray powder patterns showed almost identical values for a of the unit cells in hexagonal coordinates but the values of c are almost double and triple that of pyrosmalite respectively. These two minerals therefore were considered to be polytypes.

More recently, Donnay, Betournay & Hamill (1980) have reported a new mineral mcGillite that was described as the fifth member of the pyrosmalite group. Its chemistry is similar but not identical to that of manganpyrosmalite. This crystal has an almost identical value of a to the other members but its c axis is unusually long, being 85·97 Å which corresponds to $12c_0$. The space group of mcGillite was reported to be $R\bar{3}m$. All the people who did X-ray structure analyses on manganpyrosmalite, however, noticed that the diffraction patterns showed continuous rods of diffuse intensity parallel to **c***. These diffuse rods are observed for all values of h and k which are not multiples of 4. Because of the diffuse scattering, only isolated reflections have been used for their structure analysis, leaving some uncertainties in determination of their space group and thus in their crystal structures.

Similarly, characteristic diffuse streaks were observed in friedelite and schallerite (Takéuchi, 1980). Attempts at structure refinement on these two minerals have been made but it was found that the R values for their analysis never fell below 30%. The presence of the diffuse rods parallel to **c*** suggests frequent occurrences of stacking disorder in these layer silicate minerals, as observed commonly in other layer silicates such as the mica group (Iijima & Buseck, 1978).

To resolve the discrepancy between the true structures of these minerals and their models obtained from X-ray examination, which would give structures averaged over whole crystals, we have conducted an electron optical study on mcGillite using electron microscopy. The technique is complementary to the diffraction studies because it can provide structural details occurring in local regions of crystals on the scale of single unit cells. The usefulness of this method particularly for the study of disordered crystals has been demonstrated in numerous examples already.

2. Specimen of mcGillite

The crystal that we have examined in the present study was kindly provided by Professor G. Donnay of McGill University who described it, together with her co-workers (Donnay, Betournay & Hamill, 1980), as a new mineral 'mcGillite', the fifth member of the pyrosmalite family. The pink-colored mineral was found at the Sullivan mine, Kimberley, British Columbia. R. M. Thompson had previously examined the mineral shortly after it was first discovered nearly thirty years ago. His letter, sent to A. C. Freeze, then a district geologist at the Sullivan mine, described the structure of this mineral. It says, 'I did considerable X-ray work on this mineral this last summer. If it is friedelite, the existing data are in need of revision. This substance is *monoclinic*, *pseudo-hexagonal* and therefore cannot be isomorphous with pyrosmalite.'* His findings do not appear to have been published. The italics have been added by the present author. Dr Thompson's results are correct according to our investigation and its confirmation is the purpose of this paper.

3. Experimental procedure

The specimens for the electron microscope examination were prepared by grinding a crystal of about 1 mm size under acetone with an agate mortar and pestle. One drop of the suspension of the powdered crystal fragments was placed on a holey carbon film spread over a copper grid. The mineral has (0001) and $(01\bar{1}\bar{1})$ cleavages [indexed with reference to the published cell (Donney, Betournay & Hamill, 1980)]. Both cleavages are easy but not perfect. Thus it is easy to find crystals oriented with their basal planes nearly parallel to the incident beam direction, this being the most useful orientation for studying stacking faults of the silicate and manganese hydroxide layers in pyrosmalite. Such fragments were found and aligned with the $\langle 100 \rangle$ or $\langle 120 \rangle$ direction parallel to the incident beam direction using a double-tilt goniometer stage in the electron microscope.

The reciprocal lattices of the crystals were examined in three dimensions by tilting the crystal around several different axes, which enabled us to construct a

* This letter was made available last year by Dr J. M. Hamilton, Chief Geologist, Kimberley, at the request of Professor G. Donnay.

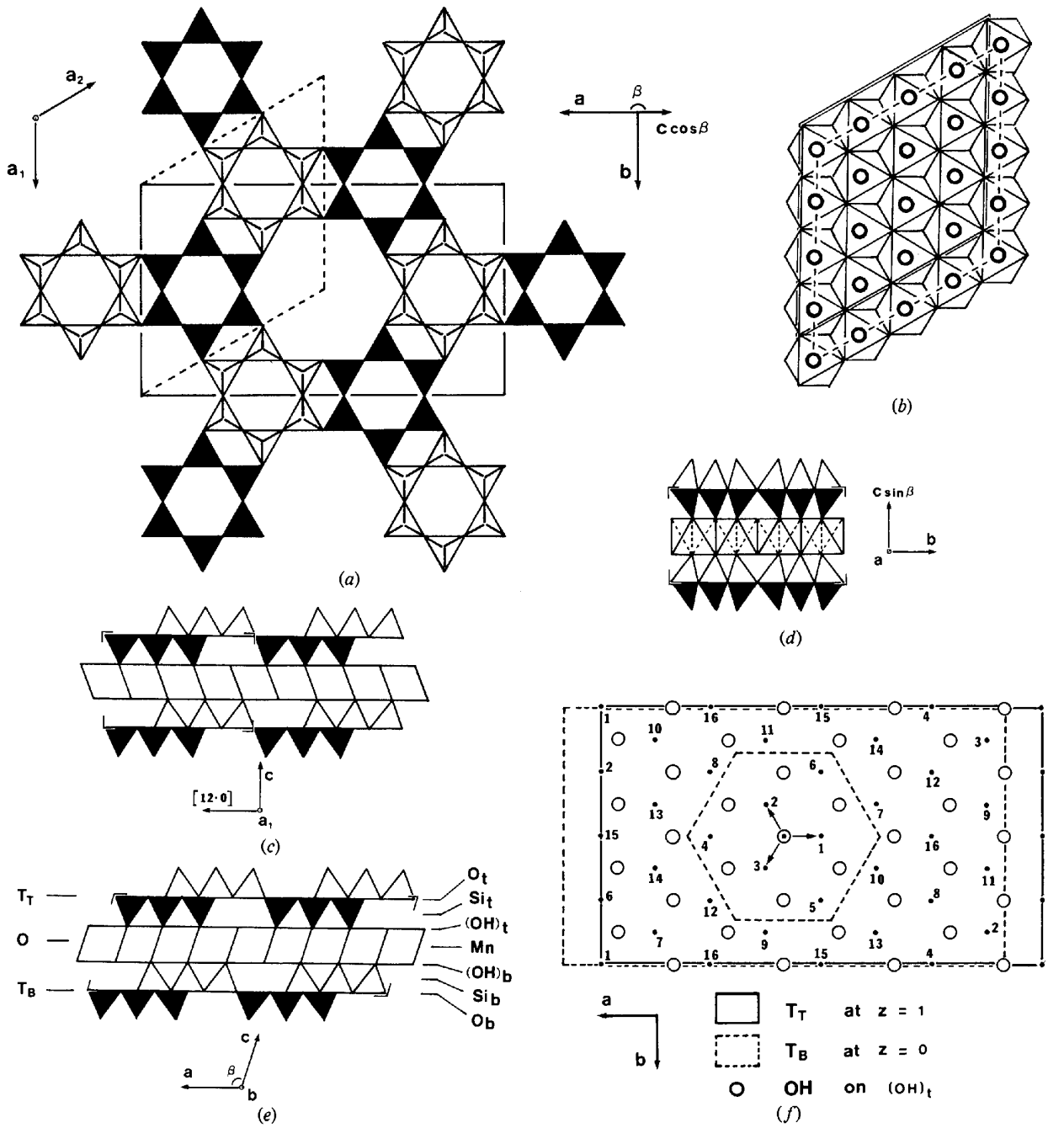

Fig. 1. (*a*) An idealized model for the sheet of SiO_4 tetrahedra of manganpyrosmalite obtained by Takéuchi *et al.* (1963). The sheet is composed of four-, six-, and 12-membered rings of SiO_4 tetrahedra which are connected by corner sharing. The open and black triangles represent tetrahedra pointing upwards and downwards respectively. The trigonal unit cell reported for manganpyrosmalite in the literature is shown by dotted lines. The new monoclinic cell proposed in the text is outlined by solid lines. (*b*) A model for the octahedral sheet of pyrochroite $Mn(OH)_2$ which alternates with the tetrahedral sheets in the structure of manganpyrosmalite. For the structure given by Takéuchi *et al.* (1963, 1969), the dotted lines should be made coincident with dotted lines in (*a*). For mcGillite the layer is shifted so that the doubled lines coincide with the dotted lines in (*a*). (*c*) A model of the trigonal structure for manganpyrosmalite viewed along **a**. (*d*) A model of the monoclinic structure (or trigonal cell) viewed along **a**. (*e*) A model of the monoclinic structure of mcGillite viewed along **b**, T_t, O, and T_B stand for a top SiO_4 tetrahedral sheet, on $Mn(OH)_2$ octahedral sheet and a bottom SiO_4 tetrahedral sheet, respectively. (*f*) The staggered arrangement of two successive tetrahedral sheets in the monoclinic structure. The dotted lines and solid lines outline the unit cell at $z = 0$ and $z = 1$ respectively. The top tetrahedral sheet is shifted by **a**/12 as shown by arrow 1. The hexagon represents a 12-membered SiO_4 ring in the tetrahedral sheet of (*a*) and open circles represent positions of OH ions on an $(OH)_T$ sheet in (*d*). Vectors connecting the center of the hexagon and small dots represent possible stacking vectors between two successive tetrahedral sheets.

reciprocal lattice from a very small region of the crystal. For this purpose, a Philips 400 electron microscope equipped with a side-entry-type tilt stage was used. Other observations were carried out by either a JEOL 100B microscope operated at 100 keV or a JEOL 200CX at 200 keV.

4. Structure type of manganpyrosmalite

The crystal structure of manganpyrosmalite proposed by Takéuchi *et al.* (1963, 1969) consists of idealized sheets of SiO_4 tetrahedra (Fig. 1*a*) and brucite-like $Mn(OH)_2$ octahedra. The network of the tetrahedra is made up of twelve-, six-, and four-membered rings, and has an overall composition $(Si_6O_{15})^{6-}$. Let us designate by T the tetrahedral network. In a 12-membered ring of the tetrahedra, a pair of adjacent tetrahedra point in the same direction. The 12-membered ring of tetrahedra has the same configuration as the one in the zeolite mordenite (Meier, 1961) with point symmetry $\bar{3}m$. The tetrahedra in the six-membered rings either all point upwards or all point downwards. The six-membered and four-membered rings have point-group symmetries $3m$ and $\bar{1}$ respectively. Kashaev (1968) reported that the six-membered rings are considerably distorted to trigonal symmetry.

The $Mn(OH)_2$ octahedral sheets designated by O (Fig. 1*b*) are centered about $z = 0$ between the two T sheets, in such a way that Mn atoms are located above the center of the 12-membered rings. To balance the charge, 12 out of 32 hydroxyl ions on the O sheet should be shared with the apical oxygen atoms on the six-membered rings as illustrated in Fig. 1(*c*). The parallelograms represent the $Mn(OH)_2$ octahedra viewed along the direction of one of the a_0 axes. The unit cell of the manganpyrosmalite, outlined by dotted lines in Fig. 1(*a*), was reported to have space group $P\bar{3}m1$ with lattice dimensions $a_0 = 13{\cdot}42$, $c_0 = 7{\cdot}159$ Å (Takéuchi *et al.*, 1969). The structure of other minerals in the pyrosmalite family are summarized in Table 1.

5. Results and interpretation

Electron diffraction patterns of mcGillite showed considerable streaking parallel to the c^* axis as expected from X-ray precession patterns. It is found, however, that some of the crystallites showed good single-crystal or only slightly streaked diffraction patterns. Diffuseness of the patterns varies from specimen to specimen. Since the rods of the diffuse scattering are elongated along the c^* axes, electron diffraction patterns taken from directions nearly parallel to the c_0 axis would always show a pseudo-hexagonal pattern.

Table 1. *Crystal data for manganpyrosmalite*

	Space group	a (Å)	c (Å)	References
McGillite	$R3m$	13·498	85·657	Donnay *et al.* (1980)
Schallerite	$P\bar{3}m1$	13·43	14·31	Bauer & Berman (1928)
Friedelite	R	13·40	21·43	Bauer & Berman (1928)
Manganpyrosmalite	$P\bar{3}m1$	13·36	7·16	Frondel & Bauer (1953)
Pyrosmalite	$P3m1$	13·35	7·15	Frondel & Bauer (1953)

In the diffraction pattern including the c^* axis, we observed most frequently four different types of patterns. Three of these patterns could not be indexed in terms of trigonal or hexagonal space groups proposed in the literature but only in terms of a monoclinic unit cell. Two of them were tentatively assumed in the principle-zone-axis orientations. In the following sections we shall describe mcGillite in terms of monoclinic structure unless otherwise stated.

Observation on a [100] *projection*

A diffraction pattern having a rectangular net of spots (Fig. 2*a*) was used for indexing other diffraction patterns. The pattern was indexed with the crystal oriented with $[03\bar{3}0]$ (referred to the trigonal cell) parallel to the incident electron beam direction. The structure projected on the $(01\bar{1}0)$ plane (Fig. 1*d*) has mirror symmetry. The figure corresponds to a [100] projection of the new monoclinic cell proposed below.

From the model shown in Fig. 1(*a*), it is likely that such a monoclinic cell could be taken as shown by a rectangle drawn with solid lines. Successive displacement of the T sheets on the (0001) plane will result in a monoclinic cell retaining one of the three mirror planes in the trigonal cell. A monoclinic cell angle β will be determined by the displacement vector. A possible structure of the monoclinic cell projected on (010) is illustrated in Fig. 1(*e*). Its (001) plane at $z = 0$ and $z = 1$ is indicated by dotted lines and solid lines respectively (Fig. 1*f*). The arrow 1 represents a displacement vector $-\mathbf{a}/12$ for the monoclinic cell. Its crystal axes are related to those of the trigonal cell as $a = \sqrt{3}a_0$ and $n = a_0$. Since the direction of the displacement is coincident with that of the [100] projection, its diffraction pattern is identical with that of the trigonal cell.

A similar stacking of the sheet silicates leading to a one-layer monoclinic structure is known as $1M$ in micas (Iijima & Buseck, 1978). In these crystals talc layers having hexagons of SiO_4 tetrahedra are arranged to give rise to a C-centered lattice. Their structural principles will be applied to the interpretation of structures of manganpyrosmalite. Using the new unit cell the diffraction pattern of Fig. 2(*a*) was reindexed to be a $0kl$ reciprocal-lattice section with $k = 2n$.

A dark-field micrograph revealed bright lines running parallel to the (001) plane (Fig. 3). They are separated by an average distance of 150 Å. A high-resolution micrograph of these lines revealed that they are stacking-fault images due to twinning occurring at a single unit-cell width. They cause weak diffuse streaks along **c*** in the diffraction patterns. Splitting of the bright lines (arrowed) suggests steps on the twin planes.

120° *rotation twinning on* (001) *planes*

On the basis of the monoclinic cell mentioned above, the electron diffraction pattern including two sets of spots shown in Fig. 2(*b*) can be described due to twinning on a (001) plane. An oblique reciprocal lattice, which cannot be explained by an one-layer trigonal cell, shares its c^* axis with the rectangular one of Fig. 2(*a*). The angle made by the two axes of the oblique lattice was measured to be 76·5°. It accords with a theoretical value 76·7° derived from our postulated monoclinic cell oriented in the [130] zone axis. This suggests that crystal I rotates by 120° on a (001) plane with respect to crystal II. It is noted that reciprocal-lattice points of crystal I, $0kl$, with $k = 4n$, are coincident with $3\bar{k}kl$ with $k = 4n$ of crystal II. Since only these reflections were employed for the X-ray structure analyses, the effects of the twinning on the diffraction intensities have been neglected.

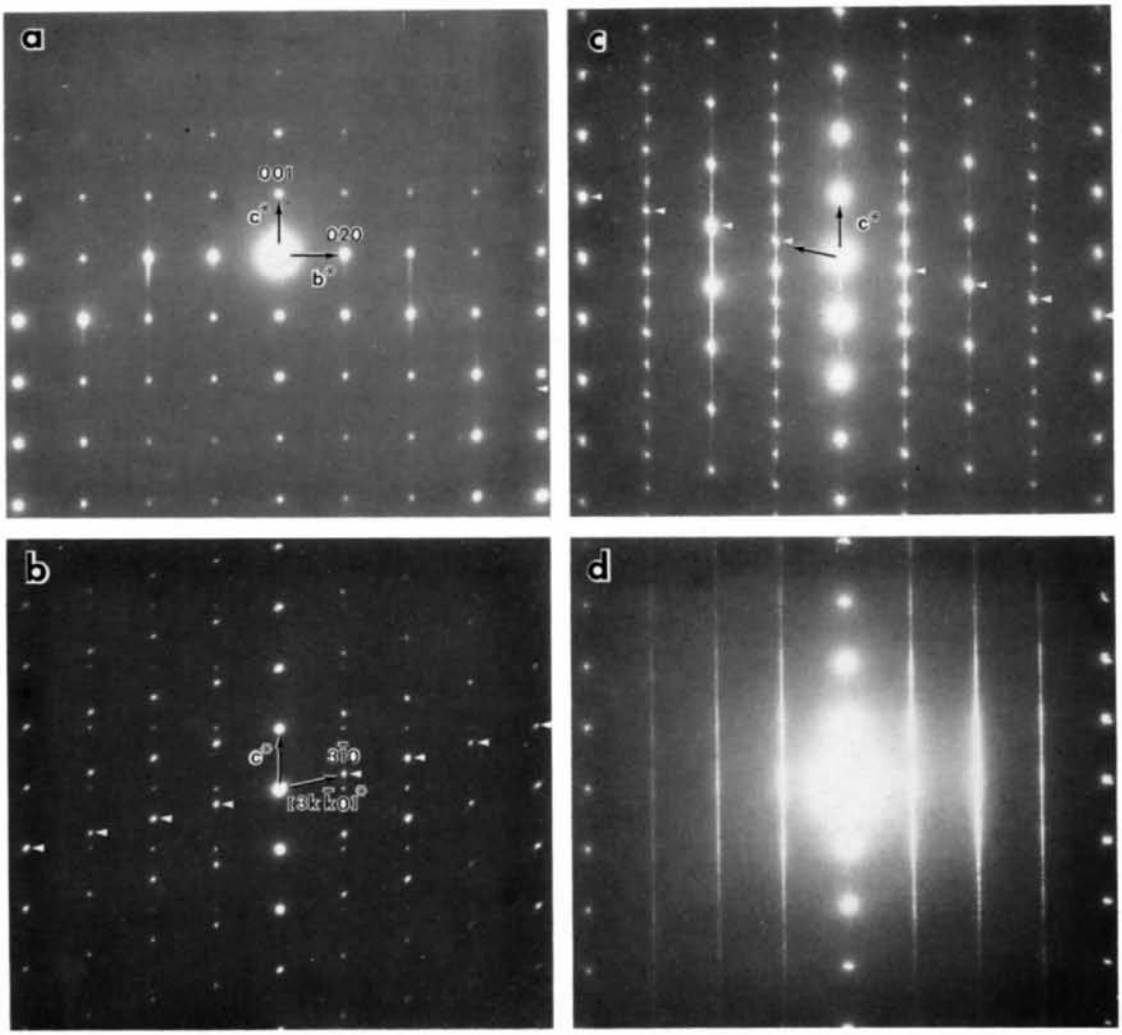

Fig. 2. Selected-area electron diffraction patterns of mcGillite. (*a*) A $0kl$ reciprocal-lattice section. (*b*) A $0kl$ reciprocal-lattice section on which a $3k\bar{k}l$ reciprocal-lattice section is superimposed. The latter spots are found to be due to the 120° rotation twin on the (001) plane. (*c*) The $3k\bar{k}l$ reciprocal-lattice section of (*b*) coexists with a $3kkl$ reciprocal-lattice section. These two sets of patterns are in the same twin relation as those of (*b*). (*d*) A $0kl$ or $3kkl$ reciprocal-lattice section showing continuous streaks at $k \neq 4n$, resulting from considerable disorders in the stacking sequence of the tetrahedral layers and the octahedral sheets in the **c** direction.

A high-resolution electron micrograph (Fig. 4) taken from the same twinned crystal as in Fig. 2(*b*) displays two twin planes indicated by arrows. An enlarged image of a twinned region (inset) reveals that a twin composition plane occurs on a single (001) plane. More details of this image will be discussed later in conjunction with disorder of the mcGillite crystal.

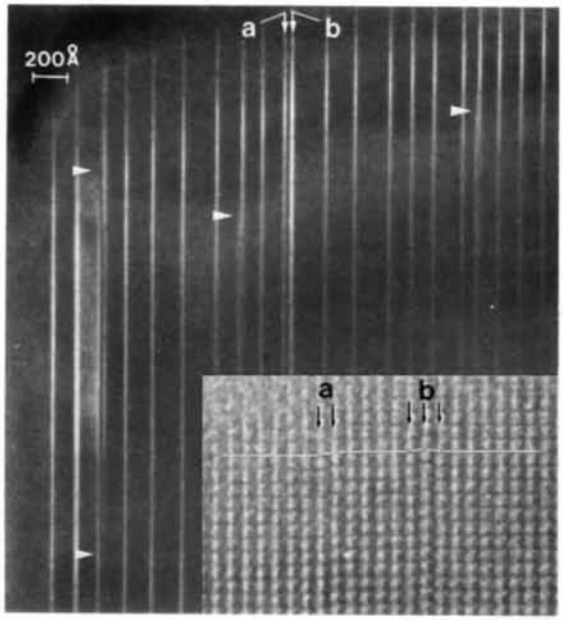

Fig. 3. A dark-field electron micrograph of a crystal of mcGillite corresponding to the electron diffraction pattern of Fig. 2(*a*). Bright lines are stacking disorders due to double (indicated by *a*) or triple twinning (indicated by *b*) occurring successively within a single width. They are indicated by arrows in the inset.

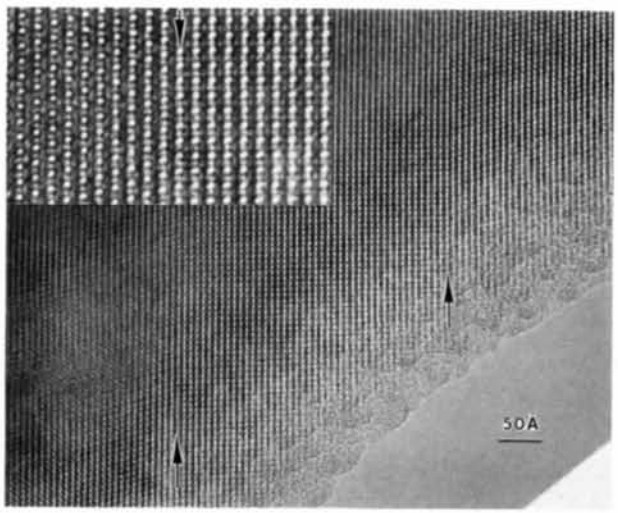

Fig. 4. An electron micrograph showing twin planes (arrowed) in a crystal of mcGillite corresponding to the electron diffraction pattern of Fig. 2(*b*). The inset is an enlarged image of a twin plane occurring on a single (001) plane. The plane is also a twin composition plane.

An electron diffraction pattern shown in Fig. 2(*c*) is also explained by the 120° rotation twin. In this instance one set of the spots corresponds to the $3k\bar{k}l$ reciprocal section but another set is mirrored with it about the c^* axis. Crystals I and II are therefore rotated by 120° clockwise and counterclockwise respectively about the c^* axis relative to the crystal oriented with its [100] axis parallel to the incident beam direction. Such rotations of the manganpyrosmalite layers can be achieved by displacing the T sheet by a vector ($\mathbf{a}/24 - \mathbf{b}/8$) or ($\mathbf{a}/24 + \mathbf{b}/8$) indicated by arrows 2 and 3 in Fig. 1(*f*). With this translation operation two twinned crystals I and II will have their common reciprocal-lattice points not only at the $00l$ reflections but also at the $3kkl$ reflections with $k = 2n$.

Diffuse streaks

A typical electron diffraction pattern showing continuous diffuse lines, frequently observed in our specimens, is represented in Fig. 2(*d*). The crystal has been aligned in the $[\bar{1}00]$ or $[\bar{1}\bar{3}0]$ zone-axis orientation. Note that these two orientations could not be determined uniquely because of the strong diffuse streaks appearing at the reciprocal lines corresponding to hkl or $3kkl$ with $k \neq 4n$.

The diffraction pattern is quite analogous to those from disordered crystals of micas or chlorites which showed continuous diffuse lines parallel to the c^* axis without diffuse streaks for reflections with $k = 3n$ (Iijima & Buseck, 1978). The origin of the diffuse streaks is understood by the fact that the stacking vectors in the talc layers has a magnitude $a/3$, where a refers to an edge of the hexagon of SiO_4 tetrahedra of the talc layer. The explanation of the diffuse streaks for disordered crystals of mica can be utilized in analysis of disordered crystals of mcGillite.

Observation on [010] *projection*

This orientation is equivalent to the $[2\bar{1}\bar{1}0]$ projection of the trigonal cell. Electron diffraction patterns in this orientation failed to show the trigonal cell but showed an oblique net of spots (Fig. 5*a*). The angle for the oblique reciprocal lattice is measured to be 74·5°.

Let us show the angle to be the angle β^* of the monoclinic structure proposed in the preceding section. The monoclinic cell outlined in Figs. 1(*a*), (*d*), (*e*) and (*f*) can be realized in the following way. When the T sheets are displaced successively, the charge balance between the T sheets $(Si_6O_{15})^{6-}$ and the O sheets $Mn(OH)_2$ imposes the situation that the number of apical oxygen atoms of the SiO_4 tetrahedra sharing with the O sheets is the same as those for the trigonal structure. This can be achieved by rotating the O sheet by 60° relative to that of the trigonal cell. Furthermore the O sheet should be situated so that the hydroxyl ions are located at the center of the 12-membered rings

which are occupied by the Mn atoms for the trigonal cell.

There are a number of possible ways of stacking two neighboring T sheets satisfying the requirement mentioned above. The structure illustrated in Figs. 1(*a*), (*d*), (*f*) is one of them. For the monoclinic structure the β can be calculated from $\beta = \tan^{-1}(\sqrt{3}a_0/12c_0) = 105{\cdot}3°$, where a_0 and c_0 are taken from Donnay's data. Thus the reciprocal angle $\beta^* = 74{\cdot}7°$. This is in excellent agreement with the experimental value.

Observation on the [110] *projection*

Other evidence supporting the monoclinic structure proposed for mcGillite was obtained by examining the $\bar{h}hl$ reciprocal-lattice section. In this projection a theoretical angle made by two axes for the oblique reciprocal-lattice net becomes 82·2°, which is again in accord with the observed value (Fig. 5*b*).

An electron micrograph taken from the same crystallite as used for the diffraction pattern of Fig. 5(*b*) displays occasional stacking faults (Fig. 6). The faulted regions have a width identical with a single layer of 7·1 Å (inset). The ($\bar{1}$10) lattice planes (indicated by a white line in the inset) are stepped across the faulted layers. The displacement parallel to the layer is about 0·9 Å. It is concluded from these experimental facts that two twin planes take place successively on (001) planes of both sides of a single unit cell as we saw in Fig. 3.

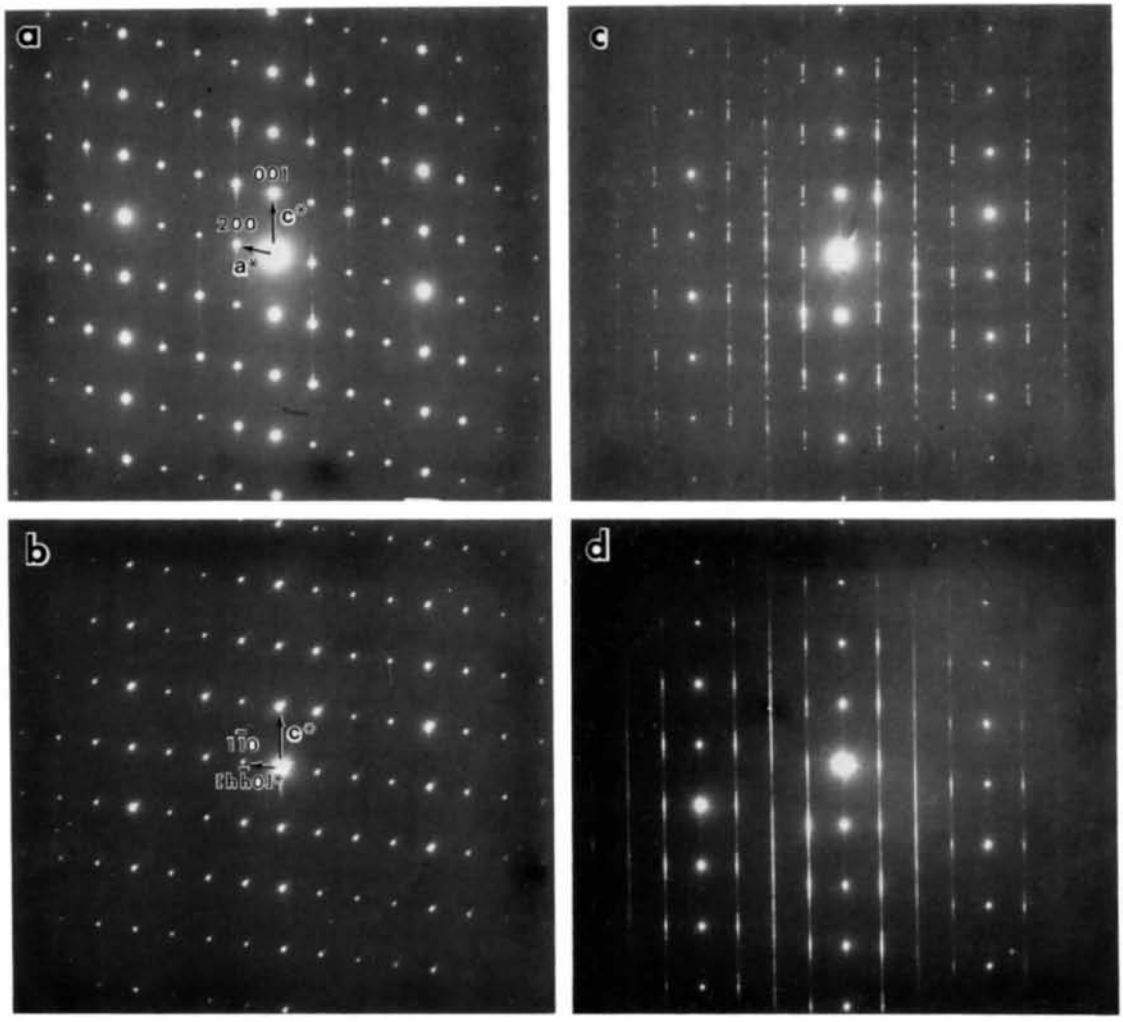

Fig. 5. Selected-area electron diffraction patterns of mcGillite. (*a*) A *h*0*l* reciprocal-lattice section. (*b*) A *hhl* reciprocal-lattice section. (*c*) A $\bar{h}hl$ reciprocal-lattice section, on which a (*h*0*l*) diffraction pattern is superimposed showing a twin of the 120° rotation type on a (001) plane. Note the latter is a mirror image of (*a*). (*d*) Disordered *h*0*l* or *hhl* reciprocal-lattice section showing diffuse streaks.

Observation on the twinning and disorder along the [010] *or* [$\bar{1}$10] *direction*

An electron diffraction pattern of the same twinned crystal as for Fig. 2(*b*) was observed, after tilting by 30° around the c^* axis, from a direction parallel to the [010] of one of the twinned crystals (Fig. 5*c*). Two different sets of spots are indexed as those obtained from superposition of the pattern of Fig. 5(*a*) and an inverted one of fig. 5(*b*). The result confirms again the occurrence of the 120° rotation twinning in the monoclinic structure.

Finally, an electron diffraction pattern showing the $h0l^*$ or hhl^* reciprocal-lattice section of a heavily disordered region of the crystal is reproduced in Fig. 5(*d*) which may be compared to that of the $3k\bar{k}l^*$ or $0kl^*$ showing diffuse streaks in Fig. 2(*d*). It is noted that reciprocal-lattice positions with $k = 4n$ are always isolated spots. This is because displacement vectors between adjacent *T* sheets are $-\mathbf{a}/12$ or its equivalent.

Summary of crystal structure

In the preceding sections we have indexed consistently all the electron diffraction patterns in terms of a monoclinic cell. Using the *T* sheet and the *O* sheet found by Takéuchi *et al.* (1963), we propose a new monoclinic cell for mcGillite. The extinction rule for the diffraction spots observed in this study is such that $h + k = 2n$ for the hkl, $h = 2n$ for the $h0l$ and $k = 2n$ for the $0k0$. This leads to space-group symmetry $C2/m$. The unit-cell dimensions are related to those of the trigonal cell by $a = \sqrt{3}a_0 = 23{\cdot}379$, $b = a_0 = 13{\cdot}498$, $c = c_0/\sin\beta = 7{\cdot}390$ Å, $\beta = \tan^{-1}(\sqrt{3}a_0/12c_0) = 105{\cdot}3°$, where $a_0 = 13{\cdot}498$, $c_0 = 85{\cdot}657/12 = 7{\cdot}138$ Å [data from Donnay *et al.* (1980)]. In order to realize the monoclinic structure, the *T* sheet must be displaced successively by a vector $-\mathbf{a}/12$, $(\mathbf{a}/24 - \mathbf{b}/8)$ or $(\mathbf{a}/24 + \mathbf{b}/8)$. The last two vectors are equivalent to the first one since individual *T* sheets have $\bar{3}m$ point symmetry.

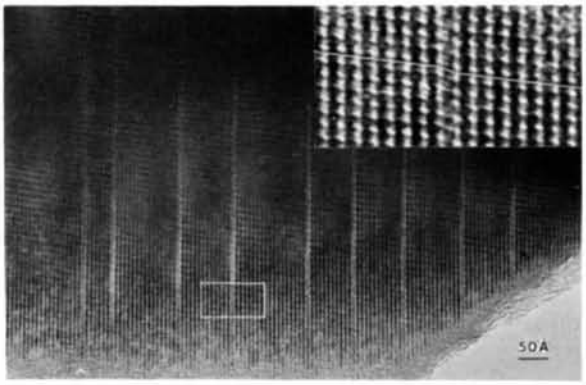

Fig. 6. An electron micrograph of a crystal of mcGillite oriented along the [110] zone axis showing occasional stacking faults. The inset is an enlarged image of one of the fault planes indicated by a rectangle. The fault is explained by occurrence of double twinning at a single unit cell.

Structure images

High-resolution electron micrographs taken from thin regions of the crystals under the condition of optimum focus are known to show approximate projections of the crystal potentials onto a plane perpendicular to the electron beam direction. The resolution of the images depends on the spherical aberration of the objective lens of the microscope. The JEOL-200CX electron microscope that we used, having a spherical aberration constant $C_s = 1{\cdot}2$ mm, has a resolution of 2·6 Å at an accelerating voltage of 200 kV. This might be sufficient to allow imaging of the positions of the individual Si and Mn ions in the [010] projection of a crystal of manganpyrosmalite. In this projection (Fig. 1*e*), the Mn ions and the Si atoms are separated by about 2·9 Å.

The electron micrograph shown in Fig. 7(*a*) is a structure image of the [010] projection. Referring to the idealized model of Fig. 1(*e*), it can be proposed that dark dots separated by 2·9 Å appearing on the lines running parallel to the (001) plane would represent individual Mn ions on the $Mn(OH)_2$ sheets. Since the Mn ions are the heaviest element in mcGillite, they should be imaged as the darkest spots in the optimum focus micrograph. The regions between the neighboring darkest lines show grey lines, which would correspond to the *T* sheets. These lines are not straight but periodically bent with a period of $a/2$. This could be explained by the arrangement of two types of SiO_4 tetrahedra pointing upwards and downwards. The bending of the grey lines could result also from distortion of the hexagonal rings of the tetrahedra, or variation of the *z* coordinates of the Si atoms. White dots appearing at both sides of the *T* sheets may be the positions of the triangular tunnels along the *b* axis shown in Fig. 1(*e*). The shift of the positions of the white dots by 1·9 Å in the neighboring two unit cells proves the monoclinic unit cell.

In the [100] projection (Fig. 1*d*), the separation of the Mn atoms is about 1·7 Å, so that they cannot be imaged separately. A structure image of this orientation (Fig. 7*b*) displays dark continuous lines that represent the *O* sheets. Grey broken lines appearing at intervals of $b/2$ between the dark lines may correspond to the groups of six SiO_4 tetrahedra, three of which are arranged as mirror images of the others and are separated by about 2 Å. The regions showing lighter contrast between the grey broken lines represent isosceles triangles where the SiO_4 tetrahedra are separated at the largest distance of about 2·7 Å in the projection of the *T* sheets. The unit cell is outlined in the micrograph. We have not calculated these images theoretically since the atom coordinates have not been refined by X-ray diffraction. Using proper atom coordinates for the monoclinic structure, we should be

able to reproduce theoretically these images. The two high-resolution micrographs described above appear to be good representations of the structures of mcGillite.

The positions of the grey broken lines in the [100] projection are arranged regularly to form a rectangular network. The insert of Fig. 4 is the same type of high-resolution image as that of Fig. 7(*b*), but it does not represent the correct crystal structure because the image was recorded from a thicker region of the crystal. Regions of grey lines are shifted at the *O* sheets indicated by arrows in the direction parallel to the (001) plane by $+1{\cdot}7$ or $-1{\cdot}7$ Å, making an oblique network which is identical to the image of the twin boundary shown in Fig. 4. Steps on (010) planes across the *O* sheet indicated by arrows are therefore caused by two successively occurring twin planes. Such a unit-cell twinning is responsible for the bright lines observed in the dark-field image of Fig. 3. It is obvious that frequent occurrences of the twinning on a unit scale causes the diffuse streaks in diffraction patterns such as Fig. 2(*d*).

(*a*)

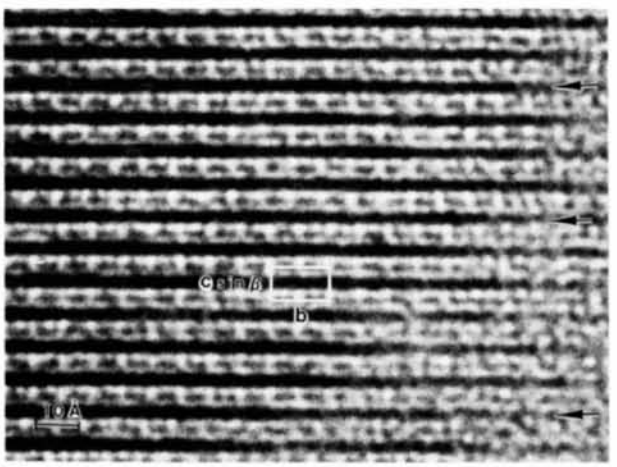

(*b*)

Fig. 7. Structure images of crystals of mcGillite. (*a*) A projection onto the (010) plane. The dark lines consisting of blobs parallel to the *a* axis represent the octahedral $Mn(OH)_2$ sheets. The blobs correspond to the positions of Mn ions separated by 2·9 Å. The white blobs appearing in two rows between the neighboring *O* sheets represent the openings in the *T* sheets of Fig. 1(*e*). Correspondingly the grey blobs represent individual SiO_4 tetrahedra. (*b*) A projection onto the (100) plane. The continuous dark lines represent the *O* sheets. In this projection the separation of Mn ions is 1·9 Å so that they are not imaged separately as in (*a*). The unit cell outlined contains two grey rods which represent groups of SiO_4 tetrahedra of the *T* layer. (See Fig. 1*d*.) Regular arrangement of rows of the grey rods perpendicular to the (001) plane is interrupted by regions indicated by arrows. Such stacking faults are caused by occurrences of double twinning at both sides of a single unit cell.

6. Discussion

McGillite revealed considerable stacking disorders and varieties of polytypes that will be reported in the following paper (Iijima, 1982). It is of interest to consider the origin of such polytypes and disorders. The formation of polytypes would not be exactly the same as that of the micas because bonding between the

Table 2. 16 *possible displacement vectors between neighboring T sheets*

Vectors are referred to the monoclinic cell proposed in the present paper. Equivalent vectors are indicated by brackets.

1	$\frac{-\mathbf{a}}{12}$
2	$\frac{\mathbf{a}}{24}-\frac{\mathbf{b}}{8}$
3	$\frac{\mathbf{a}}{24}+\frac{\mathbf{b}}{8}$
4	$\frac{-\mathbf{a}}{6}$
5	$\frac{-\mathbf{a}}{12}+\frac{\mathbf{b}}{4}$
6	$\frac{-\mathbf{a}}{12}-\frac{\mathbf{b}}{4}$
7	$\frac{-\mathbf{a}}{12}-\frac{\mathbf{b}}{8}$
8	$\frac{\mathbf{a}}{12}-\frac{\mathbf{b}}{4}$
9	$\frac{\mathbf{a}}{24}+\frac{3\mathbf{b}}{8}$
10	$\frac{-5\mathbf{a}}{24}+\frac{\mathbf{b}}{8}$
11	$\frac{\mathbf{a}}{24}-\frac{3\mathbf{b}}{8}$
12	$\frac{\mathbf{a}}{6}+\frac{\mathbf{b}}{4}$
13	$\frac{-5\mathbf{a}}{24}+\frac{3\mathbf{b}}{8}$
14	$\frac{-5\mathbf{a}}{24}-\frac{3\mathbf{b}}{8}$
15	$\frac{5\mathbf{a}}{12}$
16	$\frac{-\mathbf{a}}{3}$

T and O sheets is not purely ionic in manganpyrosmalite. We consider here some theoretically possible stacking in the one-layer T–O–T.

Two T sheets represented by T_B and T_T in Fig. 1(*e*) sandwich an octahedral $Mn(OH)_2$ sheet represented by O. The O sheet may be subdivided into an $(OH)_b$ sheet, a sheet of Mn ions and an $(OH)_t$ sheet. They have hexagonal symmetry. To describe a stacking of T_B–O–T_T, it will be sufficient to define locations of the T_T sheet relative to that of the O–T_B. The rule governing the stacking of T_T on O–T_B is such that apical oxygen atoms of the SiO_4 tetrahedra located at Si_T must share with OH ions on the $(OH)_t$ sheet. The positions of the $(OH)_t$ ions are illustrated by open circles in Fig. 1(*f*). The illustration is a projection of the monoclinic unit cell on to the (001) plane. The unit cells at $z = 0$, or the O_b sheet, and at $z = 1$, or O_t sheet, are outlined by dotted lines and solid lines respectively.

Taking the $\bar{3}m$ as an origin located at the center of the 12-membered ring in the T_B sheet illustrated by a hexagon drawn by dotted lines in Fig. 1(*f*), we define a vector for a displacement of the T_T sheet on the (001) plane. The resulting vectors connecting the center of the hexagon and the small black dots are all geometrically allowed. There are 16 such vectors, which are listed in Table 2 in terms of the monoclinic cell. Since the 12-membered ring has trigonal point symmetry, there are six non-equivalent vectors, one of which accounts for the monoclinic cell described above.

In principle, using these stacking vectors, we could have five more regular sequences of one-layer T_B–O–T_T structures. If we take a displacement vector $\mathbf{a}/6$, another monoclinic structure with lattice parameters $a = 23{\cdot}397$, $b = 13{\cdot}498$, $c = 8{\cdot}133$ Å, $\beta = 118{\cdot}6°$ and space group $C2/m$ will be obtained. Existence of this structure in mcGillite will be reported in the following paper (Iijima, 1982). Similarly, a vector $-\mathbf{a}/3$ will result in the third type of monoclinic structure.

If a stacking vector does not lie on the mirror plane for $\bar{3}m$, the structure becomes triclinic. There will be three triclinic structures for a single-layer polymorph which are described by translation vectors $(-\mathbf{a}/12 - \mathbf{b}/8)$, $(\mathbf{a}/6 + \mathbf{b}/4)$ or $5\mathbf{a}/12$, or their equivalent. At the moment we have not been successful in assigning any triclinic structure or third type of monoclinic structure. An explanation for the failure is that there is an interaction between two adjacent T_B and T_T sheets across the O sheets. Such a communication between the two T sheets has been neglected in the present discussion. In the case of the polytypism of micas, it has been suggested that some distortions existing within individual talc layers would cause the formation of multilayer polytypes of micas (Takeda & Ross, 1975).

Structural variations of multilayer polytypes of mcGillite can be described by combination of the vectors listed in Table 2. Their c^* axes are expressed by $1/nc_0$. It is noted that for multilayer structures all 16 vectors would become non-equivalent and thus a considerable number of the polytypes would be theoretically possible. We have observed polytypes in mcGillite having $n = 2$, 3, 4, 6, and 9. The c axes of the first two structures are the same as those for schallerite and friedelite (Frondel & Bauer, 1953). However, we found that they could be better described as monoclinic based on the one-layer monoclinic structure proposed in the present paper. Details of the polytypism of mcGillite will be reported in the subsequent paper (Iijima, 1982).

I would like to thank Professor G. Donnay who interested me in the problem of mcGillite and for providing the crystal. Financial support from the NSF (Grant DMR-8015785) is gratefully acknowledged. This research was also supported by the Facility for High-Resolution Electron Microscopy, established with support from the NSF Regional Instrumentation Facilities Program (Grant CHE-7916098).

References

BAUER, L. H. & BERMAN, G. (1928). *Am. Mineral.* **13**, 341–348.

DONNAY, G., BETOURNAY, M. & HAMILL, G. (1980). *Can. Mineral.* **18**, 31–36.

FRONDEL, C. & BAUER, L. H. (1953). *Am. Mineral.* **38**, 755–760.

IIJIMA, S. (1982). *Acta Cryst.* A**38**, 695–702.

IIJIMA, S. & BUSECK, P. R. (1978). *Acta Cryst.* A**34**, 709–719.

KASHAEV, A. A. (1968). *Sov. Phys. Crystallogr.* **12**, 923–924.

MEIER, W. M. (1961). *Z. Kristallogr.* **115**, 439.

TAKEDA, H. & ROSS, M. (1975). *Am. Mineral.* **60**, 1030–1040.

TAKÉUCHI, Y. (1980). Private communication.

TAKÉUCHI, Y., KAWADA, I., IRIMAGIRI, S. & SADANAGA, R. (1969). *Mineral. J.* **5**, 450–467.

TAKÉUCHI, Y., KAWADA, I. & SADANAGA, R. (1963). *Acta Cryst.* **16**, A16.